Carcinogenesis vol.30 no.1 pp.28–34, 2009
doi:10.1093/carcin/bgn240
Advance Access publication October 24, 2008

Specific association between the methyl-CpG-binding domain protein 2 and the hypermethylated region of the human telomerase reverse transcriptase promoter in cancer cells

Amandine Chatagnon[1,†], Stéphanie Bougel[2,†], Laury Perriaud[1], Joël Lachuer[3], Jean Benhattar[2] and Robert Dante[1,*]

[1]INSERM U590, Lyon F-69008, France, [2]Institut de Pathologie, Centre Hospitalier Universitaire Vaudois and University of Lausanne, Lausanne CH-1011, Switzerland and [3]ProfileXpert/Neurobiotec Service, INSERM U842, Bron F-69676, France

[*]To whom correspondence should be addressed. INSERM U590, Oncogenèse et Progression Tumorale, Centre Léon Bérard, 28 rue Laënnec, 69373 Lyon Cedex 08, France. Tel: +33 4 78 78 59 22; Fax: +33 4 78 78 27 20; Email: dante@univ-lyon1.fr

Human telomerase reverse transcriptase (*hTERT*) is expressed in most cancer cells. Paradoxically, its promoter is embedded in a hypermethylated CpG island. A short region escapes to this alteration, allowing a basal level of transcription. However, the methylation of adjacent regions may play a role in the maintenance of low *hTERT* expression. It is now well established that methyl-CpG binding domain proteins mediate the transcriptional silencing of hypermethylated genes. The potential involvement of these proteins in the control of *hTERT* expression was firstly investigated in HeLa cells. Chromatin immunoprecipitation assays showed that only methyl-CpG-binding domain protein 2 (MBD2) associated the hypermethylated *hTERT* promoter. In *MBD2* knockdown HeLa cells, constitutively depleted in MBD2, neither methyl CpG binding protein 2 (MeCP2) nor MBD1 acted as substitutes for MBD2. MBD2 depletion by transient or constitutive RNA interference led to an upregulation of *hTERT* transcription that can be downregulated by expressing mouse Mbd2 protein. Our results indicate that MBD2 is specifically and directly involved in the transcriptional repression of *hTERT* in HeLa cells. This specific transcriptional repression was also observed in breast, liver and neuroblastoma cancer cell lines. Thus, MBD2 seems to be a general repressor of *hTERT* in *hTERT*-methylated telomerase-positive cells.

Introduction

An increasing body of evidences indicate that the alterations of DNA methylation patterns are a characteristic of cancer cells (1). Generally, global reduction of DNA methylation level is associated with localized hypermethylation (1). Specifically, an aberrant hypermethylation of CpG islands at the 5′ end of tumor suppressor genes, leading to transcriptional repression, has been described both in cancer cell lines and tumor tissues (2,3).

In human epithelial and fibroblast cells, telomere shortening is a key event in replicative senescence. In >85% of cancer cells, telomere length is maintained through telomerase holoenzyme activity (4,5). Although germ cells and stem cells also exhibit high telomerase activity (4), in normal somatic cells, the catalytic subunit of the telomerase [*human telomerase reverse transcriptase* (*hTERT*)] is silenced, leading to a limited life span (6). The regulation of *hTERT* transcription has been extensively investigated and several inductors and repressors have been identified, including c-Myc, Sp1, hALP, Hif-1, Mbi-1, USF1/2, estrogen response element, p53, Mad1, myeloid-specific zinc finger protein 2, transforming growth factor-β, Wilms' Tumor 1 and CTCF (7–9). In addition, the *hTERT* promoter region is embedded in a large CpG island spanning nucleotides (nt) −1100 to +1500 from the transcription start site, suggesting that transcription of the gene might be regulated by DNA methylation.

The first studies examining the methylation status of the *hTERT* CpG island had led to a paradox. In normal somatic cells, this CpG island was found unmethylated while the gene was transcriptionally silent. However, in most of cancer cells, this region was aberrantly methylated, whereas telomerase activities and *hTERT* messenger RNAs (mRNAs) were unambiguously detected (10–13). This paradox was recently solved. *hTERT* methylation prevents the binding of negatively acting transcription factors such as CTCF inhibitor (9), and a partial hypomethylation of the *hTERT* promoter region can result in some level of transcriptional activity (14). In several cancer cell lines and tumor tissues, careful analysis of *hTERT* methylation patterns has shown that a short region of the CpG island (positions nt −165 to nt −80) is unmethylated or slightly methylated despite highly methylated border regions (14). This unmethylated region is located in the *hTERT* core promoter (positions nt −279 to nt +5) (15), and chromatin immunoprecipitation (ChIP) assays have shown that active chromatin marks are associated with this unmethylated region (16). Moreover, studies using plasmid expression vectors and patch methylation techniques indicate that the *hTERT* core promoter does not show any activity when all CpG sites are methylated (17). In contrast, the selective demethylation of a small region upstream the transcription start site significantly activates the *hTERT* promoter in a reporter plasmid. Nevertheless, the activity of the promoter under these conditions is significantly lower than when using the unmethylated core promoter. In this condition, *hTERT* does not provide a real exception to the general model of gene silencing by promoter methylation and the hypermethylation around the unmethylated region seems to play a major role in the reduction of *hTERT* transcriptional activity. Indeed, in telomerase-positive cancer cells, only 0.2–6 mRNA molecules per cell can be detected (18,19), suggesting that the transcriptional activity of the *hTERT* promoter is limited by cellular factors since high transcription rates are induced when the unmethylated promoter is used in plasmid expression vectors (14).

Transcriptional repression mediated by CpG methylation often involves methyl-CpG-binding domain (MBD) proteins. The five MBD proteins identified to date, methyl CpG binding protein 2 (MeCP2), MBD1, MBD2, MBD3 and MBD4, share a highly conserved MBD. With the exception of MBD4, which is primarily a thymine glycosylase involved in DNA repair (20), all MBD proteins are involved in the transcriptional repression mediated by DNA methylation. It has now been well established that MeCP2, MBD1 and MBD2 bind to methylated DNA and recruit different histone deacetylase complexes and histone methyl transferases, belonging to the chromatin remodeling complexes that control chromatin compaction and induce gene silencing (21–23). MBD3 lacks a functional MBD but is an integral subunit of histone deacetylase complex the Mi2–NuRD complex that is recruited through MBD2 (24,25).

These data have prompted us to investigate whether MBD proteins are involved in the repression of *hTERT* expression when hypermethylated in telomerase-positive cells.

Abbreviations: ChIP, chromatin immunoprecipitation; hTERT, human telomerase reverse transcriptase; KD, knockdown; MBD, methyl-CpG-binding domain; mRNA, messenger RNA; nt, nucleotide; PCR, polymerase chain reaction; RT, reverse transcription.

[†]These authors contributed equally to this work.

Materials and methods

Cell culture

Five human tumor cell lines, HeLa (cervical adenocarcinoma), MCF7 (breast adenocarcinoma), HepG2 (hepatocellular carcinoma), LAN-1 (neuroblastoma) and NCCIT (teratocarcinoma) and a normal human embryonic lung fibroblast

cell line, MRC5, were used in this study. Cells were obtained from the American Type Culture Collection (Rockville, MD), except for LAN-1, and grown in the medium recommended at 37°C in a humidified 5% CO_2 atmosphere.

ChIP assays

ChIP was done as described previously (26). Cross-linked chromatin was immunoprecipitated using 15 µl of two different polyclonal anti-MBD2 antibodies (kindly provided by Dr P.Wade and Dr E.Ballestar) or 20 µl of polyclonal anti-MeCP2 (Upstate Biotechnology, Lake Placid, NY), anti-MBD1 (Abcam, Paris, France) antibodies or anti-mouse IgG (Dakocytomation, Trappes, France).

Purified DNAs obtained from the input, unbound and bound fractions were quantified by densitometry using the VersaFluor™ Fluorometer (Bio-rad, Ivry, France) and RiboGreen reagent (Molecular Probes, Interchim, Montluçon, France).

Polymerase chain reaction (PCR) analysis was then performed to assess the binding of MBD proteins to the *hTERT* core promoter. An equal quantity (0.4 ng) of each DNA fraction was amplified by dose-dependent PCR (supplementary Figure S1 is available at *Carcinogenesis* Online) using HotStar Taq polymerase Kit (Qiagen, Courtaboeuf, France), 5% of dimethyl sulfoxide and 0.5 µM of primers spanning a region from nt −296 to nt −84 of *hTERT* (*hTERT* ChIP, see supplementary Table S1 available at *Carcinogenesis* Online). The thermal cycler program was 37 cycles of 94°C for 30 s, 65°C for 60 s and 72°C for 90s. PCR products were analyzed on a 2% agarose gel containing 1 µg/ml ethidium bromide and were quantified by densitometry using a Fluor's fluorimeter and Quantity One software (Bio-rad).

ChIP-on-chip

For ChIP-on-chip analysis, the specific protein–DNA complexes were obtained from independent immunoprecipitations using two different polyclonal anti-MBD2 antibodies (kindly provided by Dr P.Wade and Dr E.Ballestar). The ChIP DNAs from the input and bound fractions were amplified, labeled and hybridized on microarrays by ProfileXpert service according to Affymetrix™ protocols. Briefly, the ChIP DNA was amplified by ligation-mediated PCR. To test for enrichment of MBD2-bound sites, PCR amplification of *NBR2* (26) and *pS2* promoters was performed on each ChIP samples before and after amplification. The amplified DNAs were then labeled using the GeneChip® WT Double-Stranded DNA Terminal Labelling Kit and hybridized to the human tiling arrays (Human Promoter 1.0R Arrays), which were then washed and scanned. Raw data from the scans were analyzed using Affymetrix® Tiling Analysis Software and the results were viewed in Affymetrix' Integrated Genome Browser Software.

DNA methylation analysis

Bisulfite sequencing used to determine the CpG methylation pattern of *hTERT* promoter and proximal exonic region was performed as described previously (12,14). Briefly, bisulfite-modified genomic DNA was amplified by two primer sets [P1, positions nt −442 to nt −219 (12) and P2, positions nt −206 to nt +108 (14)] to analyze a region from nt −442 to nt +108 from the transcription start site of *hTERT*. PCR amplifications were accomplished using the master mix (Promega, Madison, WI), with the following conditions: 40 cycles of 94°C for 30 s, 54°C (P1) or 57°C (P2) for 45 s and 72°C for 50 s. DNA methylation status was then established by a direct sequencing of PCR products or by a sequencing of cloned PCR products. For the last procedure, PCR products were cloned into the pGEM-T vector using the pGEM-T vector system II (Promega). After transformation of JM109 *Escherichia coli* competent cells (Promega), plasmid DNA was extracted from clones with the QIAprep Spin Miniprep Kit (Qiagen). Each clone was sequenced with the M13 forward primer (5′-GTAAAACGACGGCCAG-3′), using a Big Dye Terminator Cycle Sequencing Kit and an ABI Prism 3100 sequencer (Applied Biosystems, Foster City, CA).

Transient transfection

siRNA duplexes for *MBD2* (sense: 5′-GGAGGAAGUGUACCGAAAATT-3′ and antisense: 5′-UUUUCGGAUCACUUCCUCCTT-3′; Eurogentec, Seraing, Belgium); non-specific small interfering RNA (siRNA) control (Eurogentec); pRev-Mbd2 (kindly provided by Dr A.Bird) (26) and pGL3 basic (Promega) were transfected in cell lines using lipofectamine 2000 (Invitrogen, Carlsbad, CA) according to the manufacturer's recommendations. Briefly, cells were seeded at 2×10^5 cells per well in six-well plates and grown to 50–60% confluence on the day of transfection. All transfections were done in Opti-MEM medium (Invitrogen) with 625 nM of MBD2 siRNA or 1 µg of Mbd2 expression plasmid. Lipofectamine 2000 complexes were incubated for 4–5 h. The medium was then removed and replaced with fresh medium. Cells were grown and harvested at various time after the transfection.

RNA extraction and reverse transcription–PCR analysis

Total RNA was extracted from cells using the RNeasy Mini Kit (Qiagen). After extraction, the integrity of total RNA was examined on a 1.2% agarose gel containing 1 µg/ml ethidium bromide and quantified by densitometry using a Fluor's fluorimeter and Quantity One software (Bio-rad) by comparison with serial dilutions of a standard RNA (Roche Molecular Biochemicals, Maylan, France).

MBD2 mRNA was quantified by competitive quantitative reverse transcription (RT)–PCR as described previously (27). *hTERT* mRNA levels were monitored by relative RT–PCR using One Step RT–PCR kit (Qiagen) and 0.1 µg of total RNA. Cycling parameters were 50°C for 30 min followed by 95°C for 15 min and then 32 cycles of 94°C for 30 s, 55°C for 60 s and 72°C for 90 s. *hTERT* transcripts were co-amplified with *PBGD* transcripts used as internal controls (for primers *hTERT* RT–PCR and *PBGD* RT–PCR, see supplementary Table S1 available at *Carcinogenesis* Online). PCR products were analyzed on a 2% agarose gel containing 1 µg/ml ethidium bromide and quantified by densitometry. The ratio between *hTERT* and *PBGD* signals was determined. To quantify more precisely *hTERT* mRNA, real-time RT–PCR was also carried out on a Rotorgene 6000 cycler (Corbett Research, Sydney, Australia) using *C. therm.* Polymerase One-Step RT–PCR System (Roche Molecular Biochemicals, Maylan, France). Each reaction mixture included 50 ng of template RNA, 250 nM of FAM-labeled probe (see supplementary Table S1 available at *Carcinogenesis* Online) and 500 nM of primers specific for *hTERT* (*hTERT* RT–PCR Q, see supplementary Table S1 available at *Carcinogenesis* Online). Cycling parameters were 60°C for 30 min followed by 95°C for 5 min and then 45 cycles at 95°C for 15 s and 60°C for 60 s. *β-Actin* mRNA levels were used to normalize *hTERT* expression. The relative level of each mRNA was calculated on the basis of two standard curves using the relative quantification method.

Results

hTERT hypermethylated CpG island is selectively associated with MBD2 in HeLa cells

To explore the potential involvement of MBD proteins in *hTERT* regulation, we have chosen cervical cancer cell line HeLa, as a first model. In these telomerase-positive tumor cells, as was shown in our earlier studies, the *hTERT* core promoter is also regionally hypermethylated (17) and might be a target of MBD proteins.

To address this issue, ChIP assays were performed using antibodies directed against MeCP2, MBD1 and MBD2. As a control, the fractions immunoprecipitated with a non-MBD protein-specific antibody (anti-mouse IgG) were also analyzed. The relative amounts of *hTERT* core promoter were determined by a dose-dependent PCR assay (supplementary Figure S1 available at *Carcinogenesis* Online) using a constant amount of DNA from each fractionation process: input, unbound and bound fractions. Representative data from at least three independent experiments are shown in Figure 1A. A strong enrichment in *hTERT* promoter was observed in the fraction immunoprecipitated by anti-MBD2 antibodies when compared with input or non-retained fractions (Figure 1A 'input', 'unbound' and 'IgG'). Since dose-dependent PCR assays were performed with a constant amount of DNA, these data strongly suggest that MBD2 is associated with the methylated region of the *hTERT* promoter. In contrast, analysis of the fractions immunoprecipitated by anti-MeCP2 or anti-MBD1 antibodies showed that these fractions were depleted in *hTERT* DNA (Figure 1A), indicating that these two proteins are not bound to *hTERT* promoter in HeLa cells. Furthermore, the depletion in *hTERT* DNA observed in the fractions bound by anti-MeCP2 and anti-MBD1 antibodies suggests that these two proteins are probably linked to other chromatin domains in HeLa cells.

Taken together, these data strongly suggest that the methylated regions adjacent to the unmethylated region of the *hTERT* core promoter are selectively associated with MBD2.

Recently, we have developed high-throughput analyses of MBD2-binding pattern using a ChIP-on-chip approach (A. Chatagnon, L. Perriaud, J. Lachuer and R. Dante, in preparation). DNAs obtained from the chromatin immunoprecipitated by anti-MBD2 antibodies were hybridized to Affymetrix Human Promoter 1.0R Array. On this chip, 25 500 human promoter regions tiled at 35 bp resolution are representing. Each promoter region covers ∼7.5 kb upstream through 2.45 kb downstream of 5′ transcription start site and for 1300 cancer-associated genes, additional 2.45 kb are also represented. Data obtained from two independent experiments performed with two different anti-MBD2 antibodies indicated that MBD2 not only bound the

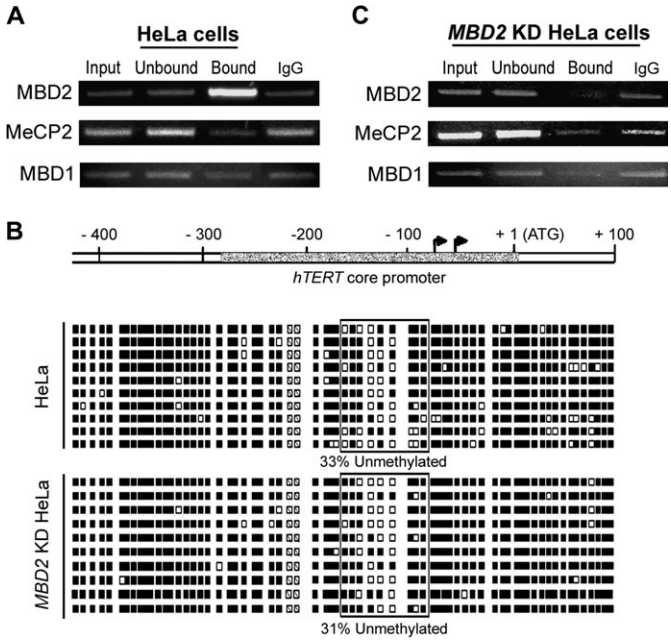

Fig. 1. MBD2 specifically binds the hypermethylated region of the *hTERT* promoter in HeLa cells. (**A**) ChIP analysis of MBD proteins binding to the hypermethylated region of the *hTERT* promoter (positions nt −296 to nt −84 from the ATG translational start site) in HeLa cells. Cross-linked chromatin was immunoprecipitated using anti-MeCP2, anti-MBD1 and anti-MBD2 antibodies or anti-mouse IgG. The relative amounts of *hTERT* core promoter were determined by a dose-dependent PCR assay using a constant amount of DNA from each step of the fractionation process: input, unbound and bound fractions. The intensities of the bands corresponding to representative PCR products amplified from the input, unbound and bound fractions are shown. (**B**) Genomic bisulfite sequencing profiles of *hTERT* promoter and proximal exonic region in wild-type HeLa and *MBD2* KD HeLa cells. A 550 bp region (positions nt −442 to nt +108) of the *hTERT* CpG island is presented on a schematic map. White dotted box, core promoter; black arrows, transcription start sites. Bisulfite-sequencing status of *hTERT* promoter and proximal exonic region is shown (number of analyzed clones for each cell line, $n = 10$). Each line represents a single-DNA template molecule. Filled and open squares, respectively, represent methylated and unmethylated CpGs. Sequencing was performed from two different regions that do not overlap (see Materials and Methods), leading to unanalyzed CpGs, barred squares. The slightly methylated region (positions nt −165 to nt −80) is framed. (**C**) MeCP2 and MBD1 do not compensate for MBD2 depletion at the *hTERT* promoter in *MBD2* KD HeLa cells. Representative examples of ChIP assays performed in *MBD2* KD HeLa cells are presented.

hypermethylated region of the *hTERT* core promoter but also covered all the hypermethylated *hTERT* CpG island (Figure 2A). As a control, results obtained for a previously identified MBD2-free hypermethylated promoter (28), *PARVG*, are also shown on Figure 2B. As expected, no MBD2-positive signal was observed along this hypermethylated promoter (Figure 2B).

The hypermethylated hTERT promoter remains free of MBD proteins in MBD2-depleted cells

In HeLa cells, among the *MBD* transcripts, *MBD2* mRNAs are the most abundant (27), suggesting that the selective binding of MBD2 to *hTERT* promoter might be due to its prominent expression. Thus, we investigated *hTERT* promoter occupancy in a HeLa clone cell line [*MBD2* knockdown (KD) HeLa cells] constitutively depleted in MBD2 by a transgene expressing a siRNA targeting the mRNA coding for this protein (26).

Quantitative competitive RT–PCR assays indicated that 89–96% *MBD2* mRNA depletion was obtained and maintained over many passages in *MBD2* KD HeLa cells. This low level of *MBD2* transcripts was correlated with a very low level of MBD2 protein, which was almost undetectable in western blot experiments (26). In addition, neither the amounts of MeCP2 and MBD1 transcripts nor the amounts of the corresponding proteins were altered by MBD2 depletion (data not shown).

As MBD2 belongs to the DNA methylation machinery, a prolonged MBD2 depletion might alter DNA methylation patterns. Therefore, the DNA methylation patterns of the *hTERT* promoter were determined in *MBD2* KD HeLa cells. DNA extracted from the cell lines was modified and amplified by PCR with primers specifically designed to amplify bisulfite-modified DNA sequence of the *hTERT* promoter and proximal exonic region. PCR fragments were cloned and sequenced. The analysis of 10 clones from wild-type HeLa cells and *MBD2* KD HeLa cells indicated that over the hypermethylated *hTERT* promoter and proximal exonic region, a small sequence (positions nt −165 to nt −80), corresponding to a part of the *hTERT* core promoter, was hypomethylated in the two cell lines analyzed (Figure 1B). Indeed, this region exhibit a low level of methylation (∼30%) but no significant difference was observed between wild-type HeLa cells and HeLa cells depleted in MBD2. Thus, the methylation patterns of the *hTERT* promoter in *MBD2* KD HeLa cells were not altered by the absence of MBD2.

As expected, in HeLa cells depleted in MBD2 proteins, ChIP assays indicated that MBD2 was no longer detected at the hypermethylated region of the *hTERT* core promoter (Figure 1C). Furthermore, this region seemed to remain free of MBD proteins since the immunoprecipitated fractions are depleted in the methylated *hTERT* promoter when anti-MeCP2 or anti-MBD1 antibodies were used in ChIP experiments (Figure 1C).

Thus, the hypermethylated region of the *hTERT* promoter is specifically targeted by MBD2 in HeLa cells and no redundancy between MBD2 and MeCP2 or MBD1 was observed at this hypermethylated region.

MBD2 depletion enhances hTERT gene transcription in HeLa cells

MBD2 is a member of the MBD protein family and their methylation-dependent repressive activities are now well established (29). Therefore, we investigated the potential involvement of MBD2 in the repression of the endogenous *hTERT* promoter in HeLa cells.

First, we determined the consequence of a transient MBD2 depletion on the expression of *hTERT* in HeLa cells. At 24 h intervals after MBD2-specific siRNA transfection, RNA was extracted and the levels of *hTERT* and *MBD2* transcripts determined by RT–PCR assays were compared with their levels in HeLa cells transfected with a non-specific siRNA. Quantitative competitive RT–PCR assays (27) indicated that a reduction of ∼90% in *MBD2* mRNA level was reached 24 h after transfection with MBD2 siRNA and maintained >96 h after transfection (Figure 3A). Western blot analysis also showed a dramatic decrease in MBD2 proteins in these cells (data not shown). In HeLa cells, 48 h after the MBD2 siRNA transfection, an elevation of 1.2-fold of *hTERT* mRNA level was observed when compared with HeLa cells transfected with a non-specific siRNA. This stimulation increased to a maximum of 1.9 at 96 h after MBD2 siRNA treatment. The expression level of *hTERT* was determined using relative RT–PCR (Figure 3A) and identical results were obtained with real-time RT–PCR for critical points (Figure 3B). It should be noted that neither the level of *MBD2* transcripts nor the level of *hTERT* transcripts were altered by non-specific siRNA transfection when compared with untreated wild-type HeLa cells (data not shown).

These data suggest that MBD2 actually represses *hTERT* expression in HeLa cells.

Stimulation of hTERT transcription in MBD2 KD HeLa cells is reversed by ectopic expression of Mbd2

The *MBD2* KD HeLa cell line offers the opportunity to investigate the functional control of the specific repression of *hTERT* by MBD2. In this cell line, MBD2 expression can be rescued using pRev-Mbd2, a vector coding for a mouse *Mbd2* RNA containing five silent point mutations and, therefore, refractory to siRNA-mediated decay (26). We also observed a 2-fold stimulation of *hTERT* expression in the *MBD2* KD HeLa cells as compared with wild-type HeLa cells (Figure 4). In these

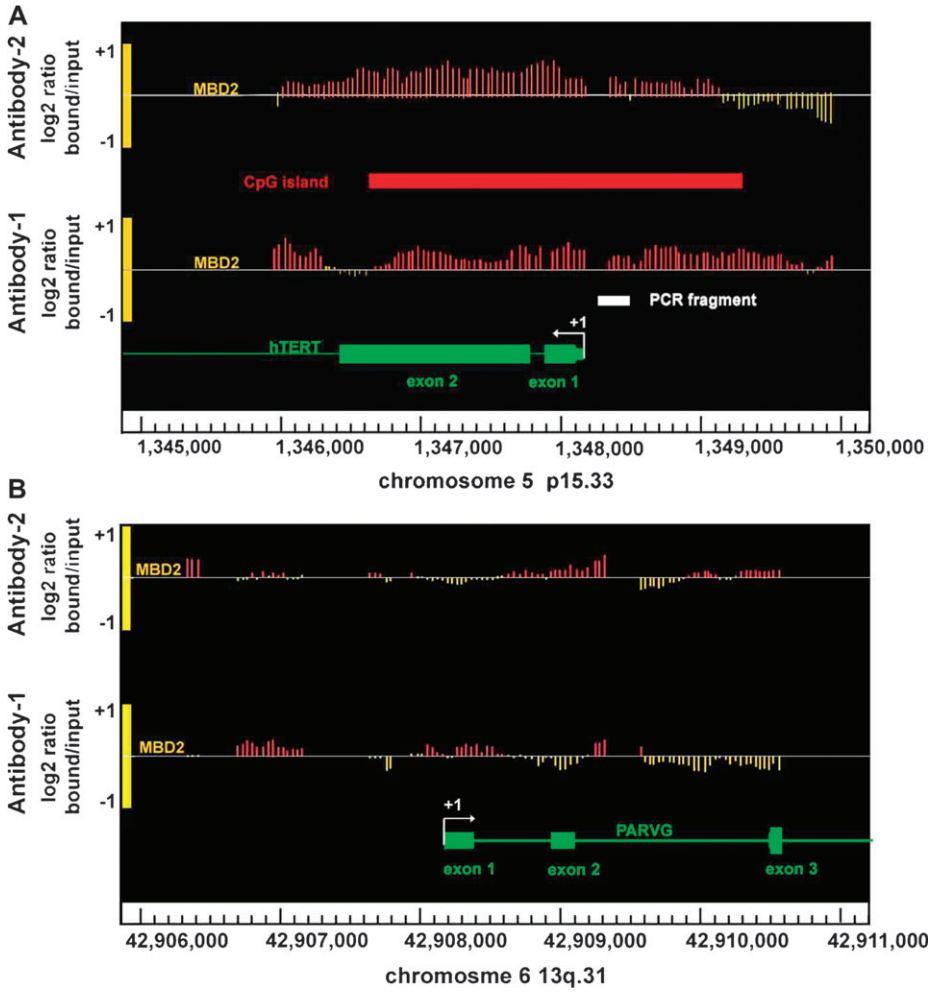

Fig. 2. ChIP-on-chip analysis of MBD2-binding sites on *hTERT* promoter. (**A**) Array peaks on *hTERT* promoter of MBD2 log2 signal ratio (MBD2/input) values are shown below the Affymetrix' Integrated Genome Browser window. Gene is transcribed from right to left. *hTERT* CpG island is shown by a red box. DNA fragment analyzed by PCR following MBD2 ChIP is represented by a white box. (**B**) *PARVG* 5′ end viewed as a MBD2-free control. Gene is transcribed from left to right.

cells, the ectopic expression of Mbd2 reduced *hTERT* transcription to a level similar to the level observed in wild-type HeLa cells (Figure 4), suggesting that MBD2 directly represses *hTERT* expression in HeLa cells. In wild-type HeLa cells, the abundance of MBD2 does not seem to be a limiting factor since the overexpression of MBD2 mediated by pRev-Mbd2 transfection did not modify *hTERT* expression level in cells containing normal amounts of MBD2 (Figure 4).

Our results demonstrate that MBD2 specifically binds to *hTERT* and represses its expression in HeLa cells.

MBD2 hTERT repression is specifically observed in hTERT-methylated telomerase-positive cancer cell lines and independent of the cellular types

Data obtained suggest that MBD2 might be a general repressor of *hTERT* transcription in *hTERT*-methylated telomerase-positive cells. In order to address this point, we tested whether the above-mentioned *MBD2* KD-mediated *hTERT* stimulation in HeLa cells could be recapitulated in other *hTERT*-methylated cell lines. A functional study was undertaken in different cell lines exhibiting characteristic *hTERT* DNA methylation patterns: (i) MCF-7, LAN-1 and HepG2 cells, three telomerase-positive cancer cell lines showing an *hTERT* core promoter unmethylated or slightly methylated despite an hypermethylated CpG island (ii) NCCIT cells, an *hTERT*-unmethylated telomerase-positive teratocarcinoma cell line and (iii) MRC5 cells, an *hTERT*-unmethylated telomerase-negative normal embryonic cell line. The *hTERT* core promoter methylation status of these cell lines and the corresponding transcript levels are shown in Figure 5. Control experiments indicated that these cell lines exhibited approximatively the same level of MBD2 transcripts ($4.8 \pm 2.7 \times 10^6$ mRNA molecules per microgram of total RNA), with the exception of NCCIT (7×10^4 mRNA molecules per microgram of total RNA).

As observed in HeLa cells, a significant decrease of *MBD2* transcripts (60–79%) was observed in the different cell lines 96 h after MBD2 siRNA transfection. Relative to the transfection with a non-specific siRNA, a ∼2-fold increase in *hTERT* mRNA was observed in all *hTERT*-methylated cell lines, LAN-1, MCF7 and HepG2 cells. In contrast, MBD2 depletion did not affect *hTERT* expression in *hTERT*-unmethylated cell lines, NCCIT and MRC5 cells (Figure 6). Since MBD2 does no bind to unmethylated DNA (24,25), these data indicate that *hTERT* induction due to MBD2 depletion is not mediated by an indirect effect.

Taken together, the specific transcriptional repression of *hTERT* by MBD2 does not seem to be restricted to a particular cancer cell line since this effect was observed in cervix, breast, liver and neuroblastoma cancer cell lines. Thus, MBD2 seems to be a general repressor of *hTERT* in *hTERT*-methylated telomerase-positive cells.

Discussion

Most (∼96%) of the CpG islands are unmethylated in normal cells (30), whereas hypermethylation of these sequences is a characteristic

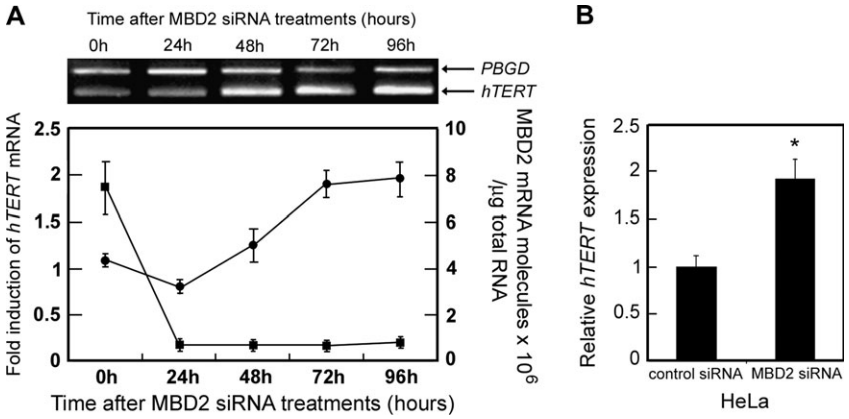

Fig. 3. Transient depletion of MBD2 proteins by MBD2-specific siRNA induces time-dependent stimulation of *hTERT* expression in HeLa cells. (**A**) HeLa cells were transiently transfected, with either MBD2 siRNA or a negative control scrambled siRNA. After 24, 48, 72 or 96 h following the transfection, RNA was extracted and the efficiency of the MBD2 siRNA treatment was determined by quantification of *MBD2* mRNA as described previously (27). *hTERT* mRNA levels were monitored by relative RT–PCR. The fold induction of *hTERT* expression was calculated from the ratio *hTERT* mRNA/*PBGD* mRNA in MBD2 siRNA-transfected cells versus scrambled siRNA-transfected cells. Mean values (± standard deviation) obtained from at least three independent transfection experiments are shown. Filled squares, *MBD2* mRNA level; filled circles, fold induction of *hTERT* mRNA. (**B**) Quantitative RT–PCR expression analysis of *hTERT* in HeLa cells 96 h after transfection with either a negative control siRNA or MBD2 siRNA. Real-time RT–PCR was done on cells lines and *hTERT* expression was normalized to β-*actin*. The relative level of each mRNA was calculated on the basis of the two standard curves using the relative quantification method. At least three independent determinations of fold differences were used to calculate the average fold difference values and associated standard deviation ($P = 0.0027$; *t*-test).

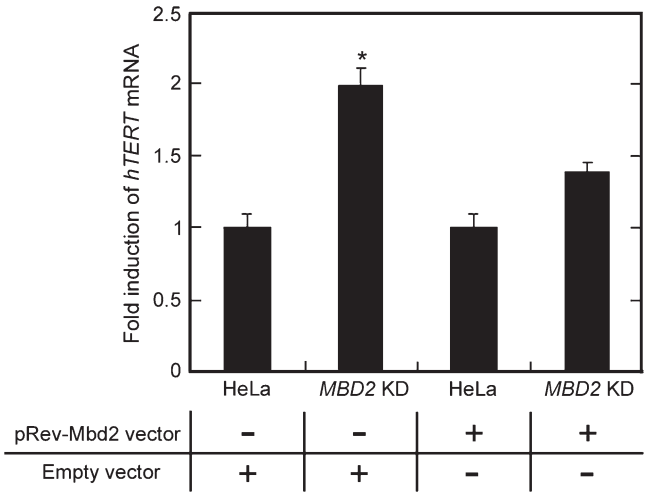

Fig. 4. Mbd2 expression rescues the reduction of *hTERT* transcript in *MBD2* KD HeLa cells. The transcriptional expression of *hTERT* was analyzed by quantitative RT–PCR 48 h after lipofectamine transfection of HeLa and *MBD2* KD HeLa cells using pRev-Mbd2, an Mbd2 vector expressing a transcript resistant to RNAi or an empty pGL3 basic vector. The relative *hTERT* mRNA in pRev-Mbd2-transfected cells or in pGL3-transfected cells or in KD HeLa cells was calculated using the same reference: the *hTERT* mRNA level in untransfected HeLa cells. Mean values obtained from at least three independent transfection experiments are shown ($P = 0.0035$, *t*-test).

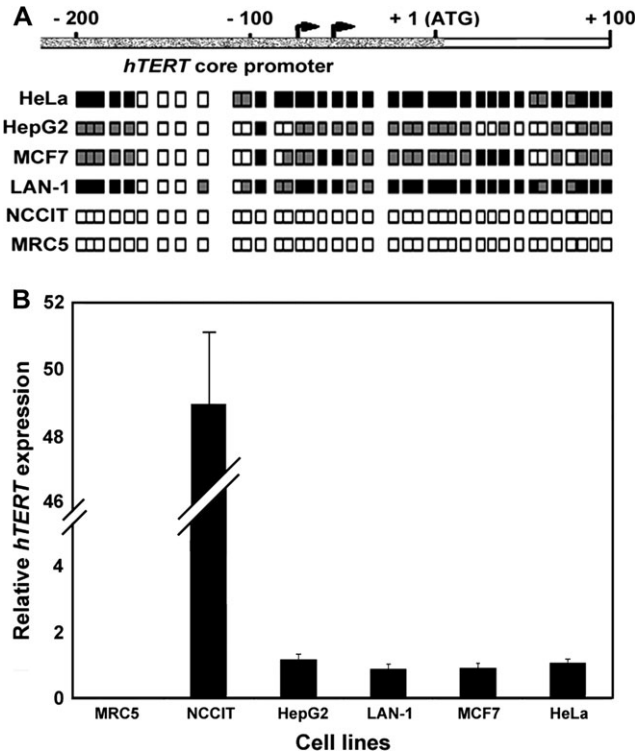

Fig. 5. DNA methylation patterns of *hTERT* and the corresponding transcript levels in different cell lines. (**A**) Bisulfite sequencing of five telomerase-positive cancer cell lines (HeLa, MCF7, HepG2, LAN-1 and NCCIT) and one normal telomerase-negative fibroblast cell line (MRC5). Bisulfite-treated DNA was PCR amplified using a primer set spanning the end of the promoter and the proximal exonic region of *hTERT*. PCR products were then directly sequenced. The analyzed 314 bp region (−206 to +108) is presented on a schematic map and results are shown for each cell lines. Filled and open squares, respectively, represent complete methylated and unmethylated CpG sites, whereas gray squares correspond to partial methylated CpG sites. (**B**) Quantitative expression of *hTERT* in MRC5, NCCIT, HepG2, LAN-1, MCF7 and HeLa cells. Real-time RT–PCR was done on cell lines, and β-*actin* was used as a reference.

of cancer cells (1). These aberrant DNA methylation patterns have been correlated with the transcriptional silencing of genes undergoing such alterations at their 5′ end CpG islands. The *hTERT* gene has provided an interesting exception since a bimodal alteration of the DNA methylation status of its 5′ end CpG island is associated with its expression in ∼85% of cancer cells and tumors tissues (4,5). The large CpG island, 2.6 kb in length, lying from nt −1102 to nt +1519 from the *hTERT* transcription, is hypermethylated at the exception of a short region (positions nt −165 to nt −80) that is unmethylated or slightly methylated despite highly methylated border regions (16,17). This particular pattern of methylation seems crucial for establishing

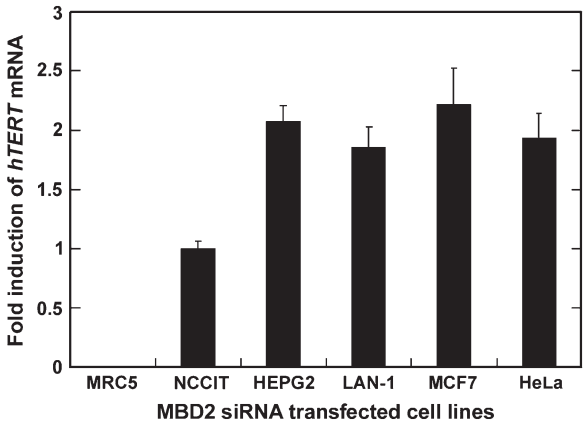

Efficiency of MBD2 siRNA	91% ± 9%	63% ± 5%	63% ± 7%	73% ± 6%	72% ± 3%	87% ± 7%

Fig. 6. Depletion of MBD2 by siRNA results in transcriptional activation of hTERT in *hTERT*-methylated telomerase-positive cancer cell lines. Fold change of *hTERT* expression between MBD2-depleted cells (MBD2 siRNA-transfected cells) and control cells (scrambled siRNA-transfected cells). *hTERT* expression was monitored by quantitative RT–PCR 96 h after transfection. Mean values (± standard deviation) obtained from at least three independent transfection experiments are shown.

hTERT expression at a basal level. Indeed, hypermethylation of CpG islands seems to be a crucial event in carcinogenesis. Thus, the methylation-free region in *hTERT* promoter may result from antagonistic pressure between the mechanisms leading to aberrant methylation and the need to keep *hTERT* expressed for unlimited life span of cancer cells.

A body of evidence has been accumulated concerning association between hypermethylation of CpG islands, transcriptional silencing and MBD-proteins binding (21). ChIP experiments and ChIP-on-chip analysis indicate that MBD2 associated the hypermethylated CpG island of *hTERT*. In this context, MBD2 seems to be a limiting factor rather than a transcriptional silencer.

Recently, a large screening of tumor suppressor gene promoters in 10 cell lines showed that human cancer cell lines tend to use a particular MBD protein (31). Furthermore, in MRC5 cells, ChIP experiments have indicated that MeCP2 and MBD2 proteins have non-overlapping binding specificities *in vivo* (23). These data, as well as our data are in favor of the 'one gene–one MBD' hypothesis, at least for some genes. Indeed, MBD2 was specifically associated with the methylated region of the *hTERT* CpG island, whereas MeCP2 and MBD1 were not detected at this locus. Moreover, MBD2 depletion did not induce MeCP2 or MBD1 binding at this methylated area in HeLa cells. Thus, the specificity of MBD proteins does not seem to be driven by their relative concentrations in a cell line, as it was suggested in an other study (31): a strong expression of a particular MBD is not necessarily associated with its preferential use in promoters.

Several studies have shown that transcriptional activation could be realized upon depletion of MBD proteins by RNA interference (RNAi) (26,28). A large-scale microarray analysis indicated that 15% of 6386 genes analyzed exhibit an increased expression change between untreated and triple MBD-depleted cells (28). It should be noted that for single-MBD interference, MBD2 depletion was the protein most commonly involved in the observed release of gene silencing by far (28). These data suggest that MBD2 plays an important role in methylation-dependent gene silencing. MBD2 depletion mediated by RNAi stimulates *hTERT* expression, either in stable KD HeLa clones or in transiently transfected HeLa cells. A 2-fold stimulation of *hTERT* expression upon *MBD2* depletion was observed, suggesting that MBD2 plays an important role in the regulation of this gene. Indeed, in human cell lines, fold changes induced by MBD2 depletion is also of the same range, 2-fold for NBR2 induced by MBD2 siRNA (26) and microarray analysis of MBD2-depleted cells exhibited a mean fold change of 7 (28). Furthermore, the fold change observed in Mbd2-deficient mouse cells is not very different from our own data. For example, it has been shown (32) that Mbd2−/− fibroblasts had 3-fold higher levels of Xist than wild-type cells. Moreover, elevated *hTERT* transcription upon MBD2 depletion is not limited to cervix (HeLa cells) since this effect was observed in breast, liver and neuroblastoma cancer cell lines. MBD2 RNAi experiments in cell lines exhibiting unmethylated *hTERT* CpG island (MRC5 and NCCIT) did not affect *hTERT* transcription indicating that MBD2 specifically and directly represses *hTERT* expression in methylation-dependent manner. Collectively, these data strongly suggest that MBD2 is a general repressor of *hTERT* expression in cancer cells.

A considerable number of transcription factors have been proposed as negative regulators of *hTERT* transcription. Nevertheless, direct evidence indicating that *hTERT* gene transcription is downregulated remains to be firmly established. Thus, MBD2 may represent a new factor directly involved in the negative regulation of *hTERT* expression. In cancer cells, MBD2 seems to play a specific role since its binding to the hypermethylated part of the *hTERT* promoter establishes a direct link between a common DNA alteration of tumor cells, CpG hypermethylation and a reduced level of *hTERT* transcription. The binding of MBD2 represents an additional layer for the control of *hTERT* expression, thereby underlying the importance of *hTERT* regulation in immortalized and cancers cells.

Supplementary material

Supplementary Figure S1 and Table S1 can be found at http://carcin.oxfordjournals.org/

Funding

Ligue Nationale contre le Cancer (Comité du Rhône and Comité de la Loire); Institut National contre le Cancer (EpiPro, CircBio, 419807-37/NG-LC); Swiss National Science Foundation (3100A0-101732, 3100A0-113505).

Acknowledgements

Conflict of Interest Statement: None declared.

References

1. Ehrlich,M. (2002) DNA methylation in cancer: too much, but also too little. *Oncogene*, **21**, 5400–5413.
2. Esteller,M. (2007) Cancer epigenomics: DNA methylomes and histone-modification maps. *Nat. Rev. Genet.*, **8**, 286–298.
3. Herman,J.G. *et al*. (2003) Gene silencing in cancer in association with promoter hypermethylation. *N. Engl. J. Med.*, **349**, 2042–2054.
4. Kim,N.W. *et al*. (1994) Specific association of human telomerase activity with immortal cells and cancer. *Science*, **266**, 2011–2015.
5. Stampfer,M.R. *et al*. (2003) Human epithelial cell immortalization as a step in carcinogenesis. *Cancer Lett.*, **194**, 199–208.
6. Yasumoto,S. *et al*. (1996) Telomerase activity in normal human epithelial cells. *Oncogene*, **13**, 433–439.
7. Goueli,B.S. *et al*. (2003) Regulation of telomerase reverse transcriptase gene activity by upstream stimulatory factor. *Oncogene*, **22**, 8042–8047.
8. Poole,J.C. *et al*. (2001) Activity, function, and gene regulation of the catalytic subunit of telomerase (hTERT). *Gene*, **269**, 1–12.
9. Renaud,S. *et al*. (2005) CTCF binds the proximal exonic region of hTERT and inhibits its transcription. *Nucleic Acids Res.*, **33**, 6850–6860.
10. Dessain,S.K. *et al*. (2000) Methylation of the human telomerase gene CpG island. *Cancer Res.*, **60**, 537–541.
11. Devereux,T.R. *et al*. (1999) DNA methylation analysis of the promoter region of the human telomerase reverse transcriptase (hTERT) gene. *Cancer Res.*, **59**, 6087–6090.
12. Guilleret,I. *et al*. (2002) Hypermethylation of the human telomerase catalytic subunit (hTERT) gene correlates with telomerase activity. *Int. J. Cancer*, **101**, 335–341.

13. Nomoto,K. *et al*. (2002) Methylation status and expression of human telomerase reverse transcriptase mRNA in relation to hypermethylation of the p16 gene in colorectal cancers as analyzed by bisulfite PCR-SSCP. *Jpn. J. Clin. Oncol.*, **32**, 3–8.
14. Renaud,S. *et al*. (2007) Dual role of DNA methylation inside and outside of CTCF-binding regions in the transcriptional regulation of the telomerase hTERT gene. *Nucleic Acids Res.*, **35**, 1245–1256.
15. Horikawa,I. *et al*. (1999) Cloning and characterization of the promoter region of human telomerase reverse transcriptase gene. *Cancer Res.*, **59**, 826–830.
16. Zinn,R.L. *et al*. (2007) hTERT is expressed in cancer cell lines despite promoter DNA methylation by preservation of unmethylated DNA and active chromatin around the transcription start site. *Cancer Res.*, **67**, 194–201.
17. Guilleret,I. *et al*. (2004) Unusual distribution of DNA methylation within the hTERT CpG island in tissues and cell lines. *Biochem. Biophys. Res. Commun.*, **325**, 1037–1043.
18. Yi,X. *et al*. (2001) Quantitation of telomerase components and hTERT mRNA splicing patterns in immortal human cells. *Nucleic Acids Res.*, **29**, 4818–4825.
19. Ducrest,A.L. *et al*. (2001) Regulation of human telomerase activity: repression by normal chromosome 3 abolishes nuclear telomerase reverse transcriptase transcripts but does not affect c-Myc activity. *Cancer Res.*, **61**, 7594–7602.
20. Hendrich,B. *et al*. (1999) The thymine glycosylase MBD4 can bind to the product of deamination at methylated CpG sites. *Nature*, **401**, 301–304.
21. Bird,A.P. *et al*. (1999) Methylation-induced repression—belts, braces, and chromatin. *Cell*, **99**, 451–454.
22. Fatemi,M. *et al*. (2006) MBD family proteins: reading the epigenetic code. *J. Cell Sci.*, **119**, 3033–3037.
23. Klose,R.J. *et al*. (2005) DNA binding selectivity of MeCP2 due to a requirement for A/T sequences adjacent to methyl-CpG. *Mol. Cell*, **19**, 667–678.
24. Ng,H.H. *et al*. (1999) MBD2 is a transcriptional repressor belonging to the MeCP1 histone deacetylase complex. *Nat. Genet.*, **23**, 58–61.
25. Wade,P.A. *et al*. (1999) Mi-2 complex couples DNA methylation to chromatin remodelling and histone deacetylation. *Nat. Genet.*, **23**, 62–66.
26. Auriol,E. *et al*. (2005) Specific binding of the methyl binding domain protein 2 at the BRCA1-NBR2 locus. *Nucleic Acids Res.*, **33**, 4243–4254.
27. Billard,L.M. *et al*. (2002) MeCP2 and MBD2 expression during normal and pathological growth of the human mammary gland. *Oncogene*, **21**, 2704–2712.
28. Lopez-Serra,L. *et al*. (2008) Unmasking of epigenetically silenced candidate tumor suppressor genes by removal of methyl-CpG-binding domain proteins. *Oncogene*, **27**, 3556–3566.
29. Klose,R.J. *et al*. (2006) Genomic DNA methylation: the mark and its mediators. *Trends Biochem. Sci.*, **31**, 89–97.
30. Weber,M. *et al*. (2007) Distribution, silencing potential and evolutionary impact of promoter DNA methylation in the human genome. *Nat. Genet.*, **39**, 457–466.
31. Lopez-Serra,L. *et al*. (2006) A profile of methyl-CpG binding domain protein occupancy of hypermethylated promoter CpG islands of tumor suppressor genes in human cancer. *Cancer Res.*, **66**, 8342–8346.
32. Barr,H. *et al*. (2007) Mbd2 contributes to DNA methylation-directed repression of the Xist gene. *Mol. Cell. Biol.*, **27**, 3750–3757.

Received August 20, 2008; revised October 3, 2008;
accepted October 11, 2008